Published in final edited form as:

FASEB J. 2020 April ; 34(4): 5563–5577. doi:10.1096/fj.201903134R.

A novel post-synaptic signal pathway of sympathetic neural regulation of murine colonic motility

Masaaki Kurahashi[1,*], **Yoshihiko Kito**[2], **Sal Baker**[1], **Libby K. Jennings**[1], **James G. R. Dowers**[1], **Sang Don Koh**[1], **Kenton M. Sanders**[1]

[1]Department of Physiology and Cell Biology, University of Nevada School of Medicine, Reno, Nevada, USA

[2]Department of Pharmacology, Saga University, Saga, Japan

Abstract

Transcriptome data revealed α1 adrenoceptors (ARs) expression in platelet-derived growth factor receptor α^+ cells (PDGFRα^+ cells) in murine colonic musculature. The role of PDGFRα^+ cells in sympathetic neural regulation of murine colonic motility was investigated. Norepinephrine, via α1A ARs, activated a small conductance Ca^{2+}-activated K^+ (SK) conductance, evoked outward currents and hyperpolarized PDGFRα^+ cells (the α1A AR-SK channel signal pathway). α1 AR agonists increased intracellular Ca^{2+} transients in PDGFRα^+ cells and inhibited spontaneous phasic contractions of colonic muscle through activation of a SK conductance. Sympathetic nerve stimulation inhibited both contractions of distal colon and propulsive contractions represented by the colonic migrating motor complexes via the α1A AR-SK channel signal pathway. Post-synaptic signaling through α1A ARs in PDGFRα^+ cells is a novel mechanism that conveys part of stress responses in the colon. PDGFRα^+ cells appear to be a primary effector of sympathetic neural regulation of murine colonic motility.

Keywords

Colonic motility; α1 adrenoceptor; Sympathetic neural regulation; PDGFRα^+ cells

[*]Corresponding author: Masaaki Kurahashi, MD & PhD, Research Assistant Professor, Department of Physiology and Cell Biology, University of Nevada School of Medicine, Anderson Medical Building MS352, Reno, NV 89557, USA, Tel: 775-784-6908, Fax: 775-784-6903, mkurahashi@med.unr.edu.

Libby K. Jennings is currently a Ph.D. student at University of Oxford, Oxford, United Kingdom, and James G. R. Dowers is currently a research scientist at ADAS, Huntingdon, United Kingdom. They were students of University of Nevada, Reno, when they were involved in this study.

Author contributions

M.K.: conception and design of experiments, collection, analysis and interpretation of data, drafting of the article and revision of the paper critically for important intellectual content. Y.K.: conception and design of experiments, collection, analysis and interpretation of data, and revision of the paper critically for important intellectual content. S.B.: conception and design of experiments, collection, analysis and interpretation of data, and revision of the paper critically for important intellectual content. L.K.J.: collection, analysis and interpretation of data. J.G.R.D.: collection, analysis and interpretation of data. S.D.K.: conception and design of experiments, interpretation of data, and revision of the paper critically for important intellectual content. K.M.S.: conception and design of experiments, interpretation of data, and revision of the paper critically for important intellectual content.

Introduction

For more than a half century, sympathetic neural regulation of the colon has been thought to be due to two types of inhibitory effects on colonic motility: pre-synaptic inhibition of the excitatory cholinergic enteric motor neurons via α2 adrenoceptors (ARs) and post-synaptic inhibition of smooth muscle contraction via β ARs (1–4). In contrast, the effects of α1 ARs on colonic motility have not been investigated in detail, because activation of α1 ARs evokes complex, either excitatory or inhibitory effects on colonic contractions (3, 5). Thus, mechanisms via α1 ARs have not been determined.

We have developed a new concept whereby the basic motor unit of gastrointestinal (GI) motility consists of smooth muscle cells (SMCs), interstitial cells of Cajal (ICC) and platelet-derived growth factor receptor α^+ cells (PDGFRα$^+$ cells), which are electrically coupled to form the SIP syncytium (6, 7). ICC and PDGFRα$^+$ cells are interstitial cells and distributed in all layers of the colon [submucosal surface of the circular muscle layer (CM), within CM, in the plane of the myenteric plexus, and within the longitudinal muscle layer (LC)] and in close proximity to neurons and nerve processes (6–9). These cells provide pacemaker activity and coordinate smooth muscle contractions by mediating neurotransduction and conveying signals to SMCs via gap junctions (6–9). Responses developed by mechanisms in any of the SIP cells can influence the integrated motor output of the SIP syncytium.

Recently through examination of cell-specific transcriptome data, we discovered that within the SIP syncytium α1 ARs, especially α1A ARs, are expressed exclusively by PDGFRα$^+$ cells in murine colon (10–12). This information suggests that PDGFRα$^+$ cells may be targets for sympathetic neural regulation. α1 ARs are G protein coupled receptors (GPCR) and linked through $G_{q/11}$ and phospholipase Cβ (PLCβ) to the increase of production of inositol 1,4,5-triphosphate (IP_3) and initiate Ca^{2+} release from intracellular stores via IP_3 receptors (13). Ca^{2+} release in PDGFRα$^+$ cells is linked to activation of small conductance Ca^{2+} activated K^+ channels (SK channels) that are expressed abundantly by these cells (14–18). Thus, it is possible that norepinephrine (NE) and/or epinephrine (Epi) activate α1A ARs and SK conductance (the α1A AR-SK channel signal pathway) in PDGFRα$^+$ cells in colon, leading to inhibitions of colonic motility. This signal pathway may be a novel inhibitory mechanism of colonic motility and a hitherto unrecognized link between stress and functional bowel disorders. Here we investigated the functional role of α1A ARs on PDGFRα$^+$ cells in sympathetic neural regulation of colonic motility.

MATERIALS AND METHODS

Animals

B6.129S4-Pdgfra$^{tm11(EGFP)Sor}$/J heterozygote mice (PDGFRα-eGFP mice), which express enhanced green fluorescent protein (eGFP) in nuclei of PDGFRα$^+$ cells throughout the body (14, 19), their wild type (WT) siblings (C57BL/6), C57BL/6-Tg(Pdgfra-cre)1Clc/J (PDGFRα-Cre mice), B6;129S-Gt(ROSA)26Sor$^{tm95.1(CAG-GCaMP6f)Hze}$/J (GCaMP6 mouse), and B6.129X1-Adra1a^{tm1Pcs}/J (*Adra1a*$^{-/-}$ mice) were obtained from Jackson Laboratory (Bar Harbor, ME). Animals (6–12 weeks *post partum*) were anesthetized by

isoflurane (AErrane; Baxter, Deerfield, IL, USA) and killed by cervical dislocation. The abdomens were opened, and colons were removed and used for experiments. Mice were maintained and the experiments performed in accordance with the National Institutes of Health Guide for the Care and Use of Laboratory Animals and the Institutional Animal Use and Care Committee at the University of Nevada, Reno, NV, approved experimental protocols.

Whole-tissue immunohistochemistry

Mouse colonic muscles were fixed in paraformaldehyde (4% w/v in 0.1 M PBS for 15 minutes at 4°C). Following fixation, preparations were washed in phosphate-buffered saline (PBS, 0.1 M, pH 7.4). Nonspecific antibody binding was reduced by incubating the tissues in 1% bovine serum albumin (BSA) for 1 hour at room temperature before addition of primary antibodies. Tissues were incubated in the primary antibody for 48 h at 4°C. Secondary antibody incubations were performed for 1 hour at room temperature. Primary antibodies: anti-PDGFRα antibody (AF1062; Dilution 1:200; R&D systems, Minneapolis, MN, USA); anti-tyrosine hydroxylase antibody (AB152; Dilution 1:500; Millipore Sigma, Burlington, MA, USA). Secondary antibodies: Alexa 594 labeled donkey anti-rabbit IgG (A-21207; Dilution 1:500; Thermo Fisher Scientific, Waltham, MA USA); Alexa 488 labeled Donkey anti-goat IgG (A-21208; Dilution 1:500; Thermo Fisher Scientific). After antibody labeling, tissues were examined with a confocal microscope (Olympus FluoView 1000; Olympus, Melville, NY, USA).

Analysis of gene expressions in PDGFRα$^+$ cells in WT mouse.

WT colonic muscles were equilibrated in Ca^{2+}-free Hank's solution and cells were dispersed as described previously (20).

Fluorescence-activated cell sorting (FACS): Dispersed cells were incubated with APC-Cy7 anti-CD45 antibody (30-F11, dilution 1:200, Biolegend, San Diego, CA, USA) and PE anti-CD140a antibody (APA5, dilution 1:200, Biolegend) followed by washing with PBS/1% FBS. Re-suspended cells had Hoechst 33258 (1 μg/mL) (BIOTIUM, Fremont, CA, USA) added as a viability marker. Cells were sorted and analysed using the BD Biosciences (San Jose, CA, USA) FACSAria II Special Order Research Product with a 130 μm nozzle with sheath pressure at 12 psi. The 355 nM laser excited Hoechst 33258 with a 450/50 nM bandpass filter. A neutral density filter was used on the forward scatter detector due to the high forward scatter properties. Cells that were CD45$^-$ CD140a$^+$ were sorted into PBC/1% FBS. Acquisition was performed on BD FACSDiva 8.0.

Isolation of total RNA and qRT-PCR: Total RNA was isolated from sorted CD45$^-$ CD140a$^+$ cells and unsorted cells using illustra RNAspin Mini RNA Isolation kit (GE Healthcare, Little Chalfont, UK). Concentration and purity of RNA were checked using an ND-1000 Nanodrop Spectrophotometer (Nanodrop, Wilmington, DE, USA), comparative amount of RNA were used for first-strand cDNA synthesized with SuperScript III (Invitrogen, Carlsbad, CA, USA), according to the manufacturer's instructions. PCR was performed with specific primers (Supplementary table 1) with Go-Taq Green Master Mix (Promega Corp., Madison, WI, USA). PCR products were analyzed on 2% agarose gels and

visualized by ethidium bromide. qRT-PCR was performed with the same primers as PCR using Fast Sybr green chemistry (Applied Biosystems, Foster City, CA, USA) on the 7900HT Real Time PCR System (Applied Biosystems).

Patch clamp experiments

Colonic muscles of PDGFRα-GFP mice were equilibrated in Ca^{2+}-free Hanks' solution and cells were dispersed, as described previously (20). The resulting cell suspension was placed in a 300-μl chamber mounted on an inverted microscope, and 10 min were allowed for cells to attach on the bottom of chamber before starting to perfuse with external solution. $PDGFR\alpha^{+}$ cells were identified by the fluorescence of eGFP in cell nuclei. Whole-cell configurations of the patch-clamp technique (perforated patch with amphotericin B) were used to record ionic currents or membrane potentials. Pipette tip resistances ranged in 5–8 MΩ. An Axopatch 200B amplifier with a CV-4 headstage (Axon Instruments, Foster City, CA) was used to measure ionic currents and membrane potentials. All data were analyzed using clampfit (pCLAMP version 10.0, Axon Instruments) and Graphpad Prism (version 6.0,Graphpad Software Inc., San Diego, CA, USA) software. External solution for whole-cell recordings was Ca^{2+}-containing physiological salt solution (CaPSS) containing (mM): 5 KCl, 135 NaCl, 2 $CaCl_2$, 10 glucose, 1.2 $MgCl_2$, and 10 Hepes adjusted to pH 7.4 with Tris. Pipette solution contained (mM): 110 K Aspartate, 30 KCl, 10 NaCl, 1 $MgCl_2$, 10 Hepes, and 0.05 EGTA, adjusted to pH 7.2 with Tris. We performed two experiments: voltage clamp experiments at a holding potential of −50 mV and current clamp experiments at $I = 0$. To analyze the data, we calculated the area under the curve (AUC) after resetting the holding current to 0 pA in voltage clamp experiments and AUC of the changes in membrane potential negative to the resting membrane potential in current clamp experiments. Values were compared for 1 min before and after applying NE.

Tension recordings of muscle strips of distal colon

Distal colon was dissected from WT and *Adra1a* KO mice and the mucosa was peeled off. Threads were tied at both end of the strips of it, and contractions of CM were measured using an isometric force transducer (model TST105A; Biopac Systems Inc., Santa Barbara, CA, USA) and the Biopac Acqknowledge software (Biopac Systems Inc.). The muscle strips were perfused with oxygenated, warmed (36°C) Krebs solution for 1 hour, and then the muscles were stretched (20–30 mN). The experimental protocols were started when the spontaneous phasic contractions (SPCs) and basal tension became consistent, about 1 hour after applying the initial stretch. To analyze the responses of SPCs to phenylephrine in the specific conditions, 4 parameters of SPCs (AUC, amplitude, tone and frequency) were measured for 5 minutes after adding phenylephrine 10 nM – 10 μM. The amplitude of SPCs was calculated as the average of the difference of tension from the bottom to the peak of the trace of SPCs and the tone was calculated as the average of the tension at the bottom of the trace of SPCs.

Ca^{2+} imaging

Colonic muscles obtained from PDGFRα-Cre-GCaMP6f mice were equilibrated with continuous perfusion of warmed KRB solution at 37°C for 1 h. Calcium Imaging was performed using a spinning-disk confocal microscopy (CSU-W1 spinning disk; Yokogawa

Electric Corporation) mounted to an upright Nikon Eclipse FN1 microscope equipped with a 60× 1.0 NA CFI Fluor lens (Nikon instruments INC, NY, USA). GCaMP6f, expressed in PDGFRα cells within colonic muscles excited at 488 nm using a laser coupled to a Borealis system (ANDOR Technology, Belfast, UK). Emitted fluorescence (>515 nm) was captured using a high-speed EMCCD Camera (Andor iXon Ultra; ANDOR Technology, Belfast, UK). Image sequences were acquired at 33 fps using MetaMorph software (Molecular Devices Inc., CA, USA) as previously described (21). All experiments were performed in the presence of atropine, L-NNA and MRS2500 to exclude effects from cholinergic, nitrergic and purinergic pathways.

Calcium event analysis: Analysis of Ca^{2+} activity in PDGFRα cells was performed, as described previously (22). Briefly, movies of PDGFRα cells Ca^{2+} activity were converted to a stack of TIFF images (tagged image file format) and imported into custom software (Volumetry G8c, GW Hennig) for initial pre-processing analysis. Tissue movement was stabilized to ensure accurate measurement of Ca^{2+} transients from PDGFRα cells. Whole cell ROIs were used to generate spatio-temporal (ST) maps of Ca^{2+} activity in individual PDGFRα cells recorded *in situ*. ST maps were then imported as TIFF files into Image J (version1.40, National Institutes of Health, MD, USA, http://rsbweb.nih.gov/ij) for *post-hoc* quantification analysis of Ca^{2+}events.

Recordings of contractions in the intact colon

The whole colon with lumber colonic nerve (LCN) and inferior mesenteric ganglion (IMG) intact was dissected from WT and *Adra1a* KO mice as shown in Fig. 5A. Threads were attached at proximal, mid and distal colon with hooks and the tensions at those 3 points were measured by three isometric tension transducers (model TST105A; Biopac Systems Inc.) with the Biopac Acqknowledge software (Biopac Systems Inc.). Electrical stimulation was applied to proximal colon as transmural nerve stimulation (TNS) and to IMG as sympathetic nerve stimulation (SNS) by bipolar platinum electrodes. For TNS and SNS, electrical stimulation was made of 0.3 ms pulse duration with 150 V. An acrylic partition was placed between the IMG and colonic wall to prevent electrical currents from directly stimulating the colonic musculature. The Krebs solution of the organ bath was perfused by a water pump (Gilson Medical Electronics, Middleton, Wisconsn, USA) and maintained at 36°C by a water bath heater (American Dade, Miami, FL, USA). The colon was left in the organ bath for 30 min and then initial tension of 30–40 mN was applied at each point of connection with the force transducers. Experimental protocols were performed 1 hour after the initial tension was applied.

Intracellular electrical recordings

The distal colon was opened along the mesenteric border. A tissue segment (about 2 cm in length) with LCN and IMG intact was pinned to a silicon rubber of a recording chamber. Conventional microelectrode techniques were used to record intracellular electrical activity from mouse distal colonic circular smooth muscle cells (CSMCs) as described previously (23). Glass capillary microelectrodes (outer diameter 1.5 mm, inner diameter 0.86 mm; Hilgenberg, Malsfeld, Germany) were filled with KCl 2 M and had tip resistances ranging between 50 and 80 MΩ. The muscle was superfused with warmed (35°C) and oxygenated

Krebs solution, at a constant flow rate of approximately 2 ml min^{-1}. Electrical responses were recorded via a high input impedance amplifier (Axoclamp-2B; Axon Instruments, CA, USA). Electrical stimulation was applied to IMG as sympathetic nerve stimulation (SNS) by platinum wire electrodes. An acrylic partition was placed between the IMG and colonic wall to prevent current from making noises and directly stimulating enteric neurons in the recording of intracellular electrical activity. All experiments were performed under the existence of nifedipine 3 μM.

Reagents

Norepinephrine-bitartrate salt, phenylephrine hydrochloride, atropine, N_{ω}-Nitro-L-arginine methyl ester hydrocloride (L-NNA), Hexamethonium chloride, propranolol hydrochloride, substance P acetate salt hydrate, 18β-Glycyrrhetinic acid, and prazosin hydrochloride were obtained from Millipore Sigma (Burlington, MA, USA). MRS2500 (selective antagonist of P2Y1 receptor), RS100329 (selective antagonist of α1A adrenoceptors), α-Yohimbine hydrochloride (Rauwolscine) (antagonist of α2 adrenocoptors), [D-p-Cl-Phe^{6},Leu^{17}]-VIP (VIP inhibitor), and PACAP 6–38 2 μM (PACAPi) were obtained from Tocris Bioscience (Ellisville, MO, USA). Tetrodotoxin citrate (TTX) was obtained from abcam (Cambridge, United Kingdom). Apamin (selective SK channel inhibitor) was obtained from Santa Crus Biotechnology (Dallas, TX, USA).

Statistical analyses

Data are expressed as means ± SE of n cells. All statistical analyses were performed using Graphpad Prism. We used paired *t*-test, non-paired *t*-test, or one-way ANOVA to compare groups of data. In all statistical analyses, $P < 0.05$ was considered statistically significant.

Results

PDGFRα^{+} cells are capable of responding to sympathetic neural input via α1A ARs and SK conductance

The anatomical relationship between sympathetic nerve fibers and PDGFRα^{+} cells was investigated using whole-mount immunolabeling with antibodies against tyrosine hydroxylase (TH), which is a marker of sympathetic nerve fibers, and PDGFRα (Fig. 1A). PDGFRα^{+} cells were found in close proximity to sympathetic nerve fibers within the circular muscle (CM) layer (Fig. 1Aa) and in the plane of the myenteric plexus (Fig. 1Ab).

Gene expression study was performed to validate the RNA-seq data (10–12). PDGFRα^{+} cells were isolated from wild type (WT) mouse colonic muscles, labelled with anti-PDGFRα antibody and collected by fluorescence activated cell sorting (FACS). Gene expression was analyzed by qPCR (Fig. 1B) and the sorting efficacy of FACS was validated by checking cell-specific markers: *Pdgfra*, *Myh11* (SMC marker), *Kit* (ICC marker), *Uchl1* (neuronal marker), *Kcnn3* (SK3 channels; PDGFRα^{+} cells marker) and *P2ry1* (a purinergic receptor highly expressed by PDGFRα^{+} cells). The expression profiles of those genes in sorted PDGFRα^{+} cells were consistent with previous reports (16). Relative expression ratio of *Adra1a*, *Adra1b* and *Adra1d* to the house keeping gene *Gapdh* in PDGFRα^{+} cells were 0.20 ± 0.01, 0.048 ± 0.002 and 0.00 ± 0.00 (n = 3) respectively, whereas the ratio of

transcripts of those genes to *Gapdh* in unsorted cells, which were the dispersed cells of colonic muscle before performing FACS, were 0.011 ± 0.002, 0.0025 ± 0.0002 and 0.0031 ± 0.0002 (n = 3) respectively. Therefore, we confirmed that α1 ARs, especially α1A ARs, were enriched in PDGFRα$^+$ cells.

Sympathetic transmitter-mediated responses via α1A ARs in PDGFRα$^+$ cell were examined using the patch clamp technique (Fig. 1C–E). Single PDGFRα$^+$ cell dispersed from PDGFRα-eGFP mouse colon was held under the voltage-clamp at the holding potential of −50 mV and norepinephrine (NE) (10 μM) was applied repeatedly (Fig. 1C and 1D). NE evoked transient outward currents, which were significantly inhibited by RS100329 (100 nM), a selective α1A AR antagonist (24) (Fig. 1C; n = 5; average reduction 90.64 ± 3.43 %; $P < 0.0001$), or by apamin (300nM), an SK channel antagonist (Fig. 1D; n = 5; average reduction 82.82 ± 3.38 %; $P < 0.0001$). Under the conditions of these experiment (ionic gradients and the holding potential), only K^+ conductance is expected to generate outward currents, and, therefore, these data support the conclusion that PDGFRα$^+$ cells express functional α1A ARs and binding of NE to α1A ARs opens SK channels on PDGFRα$^+$ cells (the α1A AR-SK channel signal pathway). The average of AUC (pA•min) for 1 min before and after applying NE in the experiments as shown in Fig. 1C were 1.07 ± 0.24 and 24.45 ± 12.16, respectively, which were reduced to 1.02 ± 0.26 in the presence of RS100329 (n = 5). The average of AUC (pA•min) for 1 min before and after applying NE in the experiments as shown in Fig. 1D were 1.14 ± 0.30 and 38.95 ± 17.04, respectively, which were reduced to 5.57 ± 2.10 in the presence of apamin (n = 5). Activation of outward current would be expected to hyperpolarize the membrane potentials of the cell, and we validated, by performing current clamp experiments ($I = 0$), that NE (10 μM) hyperpolarized PDGFRα$^+$ cells (Fig. 1Ea; n = 6). RS100329 (100nM) blocked the hyperpolarization evoked by NE (Fig. 1Ea and 1Eb; n = 6). The averages of ΔAUC (mV•min) (AUC for 1 min after applying NE - AUC for 1min before applying NE) for 1 min in response to NE in the experiments as shown in Fig. 1E were −18.28 ± 11.66, which were reduced to −0.057 ± 0.11 in the presence of RS100329 (n = 6).

NE evokes Ca^{2+} transients in PDGFRα$^+$ cells via α1A ARs

Confocal imaging was used to monitor Ca^{2+} dynamics in PDGFRα$^+$ cells and evaluate cell-specific responses to NE in the colon. Imaging was performed on flat sheets of distal colonic muscle from PDGFRα-Cre-GCaMP6f mice. Spindle shaped PDGFRα$^+$ cells were found in the circular muscle of the colon running parallel to the muscle fibers, as previously described (25) and shown in Fig. 2A and 2B. Ca^{2+} transients were resolved under basal conditions in PDGFRα$^+$ cells within a given field (discrete, localized Ca^{2+} transients occurred in 14.4 ± 5% of cells at an average of 6.8 ± 1.8 events min^{-1} (range 1–10 events min^{-1}; $n = 5$). Spontaneous Ca^{2+} transients were not resolved in the remaining PDGFRα$^+$ cells. These Ca^{2+} transient parameters are consistent with the Ca^{2+} events described previously in PDGFRα$^+$ cells loaded with the Ca^{2+} indicator Oregon green (25). First, we confirmed that the GCaMP6f signals occurred in PDGFRα$^+$ cells by testing a specific P2Y1 receptor agonist (MRS2365; 1 μM) (26). P2Y1 receptors are highly and exclusively expressed in PDGFRα$^+$ cells in muscle bundles, so responses to this agonist constitute a signature for PDGFRα$^+$ cells (14, 16, 17, 25). MRS2365 elicited Ca^{2+} transients in PDGFRα$^+$ cells (Fig.

2D). Then we tested whether NE evoked Ca^{2+} transients in PDGFRα$^+$ cells in the presence of atropine (1 μM), L-NNA (100 μM), and MRS2500 (1 μM), to reduce contamination from cholinergic, nitrergic and purinergic responses respectively. NE (10 μM; Fig. 2 C and 2E) significantly increased the frequency of Ca^{2+} transients in PDGFRα$^+$ cells from 2.9 ± 1.1 to 68.9 ± 4.6 min^{-1} (Fig. 2G; P= 0.0001, c = 23, n = 5) min^{-1}. NE increased all Ca^{2+} transients parameters tabulated, including Ca^{2+} transient area (Fig. 2H, P = 0.0046, c = 23, n = 5), duration (Fig. 2I, P = 0.003, c = 23, n = 5) and Ca^{2+} spatial spread (Fig. 2J, P = 0.002, c = 23, n = 5). Pretreatment of colonic muscles with RS100329 (100 nM) did not affect basal Ca^{2+} transient activity in PDGFRα$^+$ cells, except a small increase in the spatial spread of Ca^{2+} transients (Fig. 2J, P = 0.02, c = 23, n = 5). However, NE in the presence of RS100329 (100 nM) failed to evoke Ca^{2+} responses in PDGFRα$^+$ cells, as compared to control conditions in Ca^{2+} transient area (Fig. 2H, P = 0.42, c = 23, n = 5), duration (Fig. 2I, P = 0.51, c = 23, n = 5) and spatial spread (Fig. 2J, P = 0.87, c = 23, n = 5). A small increase in frequency of Ca^{2+} events was, however, observed (Fig. 2G, P = 0.04, c = 23, n = 5).

α1 AR agonist inhibits contractions of distal colon via the α1A AR-SK channel signal pathway in PDGFRα$^+$ cells.

We next sought to understand the impact of the α1A AR-SK channel signal pathway in PDGFRα$^+$ cells on distal colonic muscle contractions. Therefore, intracellular electrical recordings and contractile experiments of circular muscle of distal colon were performed. Tetrodotoxin (TTX; 1 μM) was included in the solution bathing the colonic muscles to emphasize post-synaptic responses to an α1 AR agonist, that is, responses developing in the SIP syncytium.

In intracellular electrical recordings, the membrane potentials of circular SMCs of distal colon were hyperpolarized by PE (1 μM; n = 10; left panel in Fig. 3A) and PE (10 μM; n = 12; right panel in Fig. 3A) and the effects of PE (10 μM) were blocked by RS100329 (100 nM; Fig. 3B; n = 6) or apamin (300 nM; Fig. 3C; n = 6). The summary of intracellular electrical recordings is shown in Fig. 3D. The values of ΔV (mV) induced by PE (1 μM), PE (10 μM), RS + PE (10 μM), Apa + PE (10 μM) are −3.17 ± 0.38, −15.05 ± 0.61, −0.09 ± 0.35, −1.01 ± 0.28, respectively.

In contractile experiments of circular muscle of distal colon, PE inhibited the amplitude of spontaneous phasic contractions (SPCs) in a concentration-dependent manner (Fig. 4Aa; n = 5). RS100329 (100 nM; Fig. 4Ab; n = 6) or apamin (300 nM; Fig. 4Ac; n = 5) blocked the effects of PE on SPCs. *Adra1a*$^{-/-}$ mice, with the gene encoding α1A ARs deactivated, had no compensatory expression of the other α1 ARs (Supplementary Fig. 1). The inhibitory effects of PE on SPCs of distal colon almost disappeared in *Adra1a*$^{-/-}$ mice (Fig. 4Ad; n = 6). Summary showing 4 tabulated parameters of contractile activity in muscle strips of the distal colon, AUC (Fig. 4Ba), amplitude (Fig. 4Bb), tone (Fig. 4Bc) and frequency (Fig. 4Bd) of SPCs are depicted in Figure 4B. The actual values of the 4 parameters are shown in Supplementary Table 2. The inhibitory effects of α1A ARs were most prominent on the amplitude of SPCs (Fig. 4Bb). These data validated the fact that the hyperpolarization evoked by the α1A AR-SK channel signal pathway in PDGFRα$^+$ cells exerted an inhibitory effect on contractions of the distal colon.

Sympathetic nerve stimulation (SNS) inhibits distal colonic contractions via the α1A AR-SK channel signal pathway in PDGFRα$^+$ cells.

We also investigated the consequences of NE release from sympathetic neurons using a preparation with connections to the lumber colonic nerve (LCN) and the inferior mesenteric ganglion (IMG) intact. This preparation allowed stimulation of IMG and activation of sympathetic neurons innervating the colon (hence called sympathetic nerve stimulation; SNS), without interference from activation of enteric neurons (Fig. 5A). To investigate the post-synaptic effects of endogenous NE on the SIP syncytium, antagonists of all major enteric motor neurotransmitters, atropine (1 μM), L-NNA (100 μM) and MRS2500 (1 μM) were included in the bath solutions. Hexamethonium (100 μM), a ganglionic antagonist was also included (presence of these antagonists is abbreviated as ALMH in the text and figures). Under these conditions, SNS inhibited contractions of distal colon (Fig. 5Ba and 5Ca; n = 23). These inhibitory responses were not abolished by the β AR antagonist, propranolol (10 μM; Fig. 5Bb and 5Cb; n = 6), but RS100329 (100 nM) + propranolol (Fig. 5Bc; n = 10) or apamin (300 nM) + propranolol (Fig. 5Cc; n = 5) blocked the inhibitions evoked by SNS. Fig. 5D shows a summary of the responses to SNS, in which inhibitory responses of colonic contractions elicited by SNS (ΔAUC) were not blocked by a single antagonist (e.g. RS100329, propranolol, or α2 AR antagonist α-Yohimbine), but were completely blocked by combination of RS100329 + propranolol or apamin + propranolol. The inhibitory responses of colonic contractions to SNS in *Adra1a*$^{-/-}$ mice were blocked by propranolol (10 μM) alone (Fig. 5E; n = 5).

Hyperpolarization induced by activation of SK channels on PDGFRα$^+$ cells conducts to SMCs through gap junctions (25). Therefore, we also tested the effect of a gap junction inhibitor, 18β-glycyrrhetinic acid, on the inhibition of contractions caused by SNS via α1A ARs on PDGFRα$^+$ cells. For this experiment, we used substance P (1 μM) to enhance contractions of distal colon and to prevent 18β-glycyrrhetinic acid from weakening contractions to such an extent that it would be impossible to estimate the inhibitory effects of SNS. And, also, we used ALMH + propranolol (10 μM) to isolate the responses mediated by α1 ARs on PDGFRα$^+$ cells. Under this condition, the inhibition of contractions caused by SNS (Fig. 5Fa) was completely blocked by 18β-glycyrrhetinic acid (100 μM; Fig. 5Fb and 5Fc; n = 6). The values of ΔAUC (mN•min) by SNS of each protocol are described in Supplementary Table 3.

Intracellular recordings of the membrane potential were recorded from circular SMCs of distal colon in a preparation with LCM and IMG intact. SNS induced hyperpolarization composed of fast and slow components (Fig. 5Ga and 5Ha; n = 12). An α1 AR antagonist, prazosin (1 μM; Fig. 5Gb; n = 6), or apamin (300 nM; Fig. 5Hb; n = 6) inhibited the fast component of the hyperpolarization, and propranolol (10 μM; Fig. 5Gc and 5Hc; n = 6 for each of protocol) inhibited the remaining slow component of hyperpolarization. Fig. 5I shows summary illustrating the effects of SNS on the membrane potential of circular SMCs. SNS-induced hyperpolarization (ΔV) was significantly inhibited by prazosin or apamin and totally blocked by prazosin + propranolol or apamin + propranolol. The values of ΔV (mV) by SNS of each protocol are exhibited in Supplementary Table 4.

Additionally, in the presence of α2 AR antagonist α-Yohimbine (100nM) and β AR antagonist propranolol (10 μM), responses of distal colon to SNS without ALMH (Supplementary Fig. 2Aa) were not different from responses with ALMH (Supplementary Fig. 2Ab and 2Ac; n = 5), suggesting that the functional expression of α1 ARs in enteric motor neurons is marginal. This conclusion is consistent with gene expression data in Fig. 1B. It should also be noted that in the presence of ALMH antagonists, responses of the distal colon to SNS (Supplementary Fig. 2Ba and 2Ca) were not affected by a VIP antagonist, [D-p-Cl-Phe^{6},Leu^{17}]-VIP (1 μM; Supplementary Fig. 2Bb and 2Bc; n = 4) or a PACAP antagonist, PACAP 6–38 (2 μM; Supplementary Fig. 2Cb and 2Cc; n = 5), suggesting that enteric inhibitory peptides, VIP and PACAP are not involved in the inhibitory responses of distal colon to SNS.

SNS inhibits the colonic migrating motor complexes (CMMCs) via α1A ARs on PDGFRα^{+} cells.

We investigated the functional role of α1A ARs on PDGFRα^{+} cells with respect to generation and propagation of CMMCs representing propulsive contractions of colon (27, 28). These experiments were performed without any neurotransmitter antagonists, with an α1A AR antagonist or in *Adra1a*$^{-/-}$ mice to determine the relative potency of α1A ARs in sympathetic neural regulation of CMMCs, using the same preparation shown in Fig. 5A. Transmural nerve stimulation (TNS) at the proximal colon initiated CMMCs from proximal to distal colon as indicated by * in Fig. 6Aa. Those CMMCs were inhibited at mid and distal colon by SMS (2 Hz) (Fig. 6Ab; n = 5). The contraction of proximal colon was not affected significantly by SNS, which suggested the sympathetic nerve fibers originating from IMG might innervate mid and distal colon primarily. RS100329 (100 nM) attenuated the inhibitory effects of SNS (Fig. 6Bb and 6C; n = 5). The values of amplitude (mN) of each condition are described in Supplementary Table 5. Intracellular electrical recordings were performed to verify whether SNS (2Hz) hyperpolarized membrane potentials of circular SMCs of distal colon via α1 ARs (Supplementary Fig. 3). SNS (2Hz) hyperpolarized membrane potentials of SMCs (Supplementary Fig. 3Aa) and this response was blocked by prazosin (1 μM) (Supplementary Fig. 3Ab and 3B; n = 5).

The role of α1A ARs in PDGFRα^{+} cells in regulating spontaneous CMMCs was also investigated (Fig. 6D and 6E). SNS (2Hz and 5Hz; 10 min) was applied to IMG. SNS caused minor inhibition of CMMCs in the proximal colon, but blocked progression of CMMCs through mid and distal colon of WT mice (Fig. 6Da; n = 9). However, SNS had no effects on CMMCs in *Adra1a*$^{-/-}$ mice (Fig. 6Db; n = 8). Summary are provided in Fig. 6E and illustrate the significant effects which SNS had on CMMCs when α1A ARs are available in colonic muscles. The values of amplitude (mN) of each protocol are described in Supplementary Table 6.

Sympathetic neural regulation of colonic motility has also been linked to pre-synaptic inhibition of cholinergic excitatory motor neurons via α2 ARs (4). Therefore, we compared the effects of the blockade of cholinergic neurotransmission and SNS on regulation of CMMCs (Supplementary Fig. 4). Atropine (1 μM) reduced the amplitude of CMMCs

(Supplementary Fig. 4a and 4b; n = 5), but the blockade of cholinergic neurotransmission produced far less inhibition of CMMCs than SNS (Fig. 6E and Supplementary Fig. 4c).

Discussion

Colonic motility is controlled by neural inputs from the enteric nervous system and both sympathetic and parasympathetic divisions of the autonomic nervous systems. Autonomic neurons provide inhibitory and excitatory regulation of colonic motility (29), and it has been proposed that constipation predominant irritable bowel syndrome (IBS-C) is associated with parasympathetic dysfunction and diarrhea predominant IBS (IBS-D) may be related to sympathetic dysfunction (30). Possible involvement in colonic motility disorders makes it important to understand mechanisms by which autonomic neurons regulate colonic motility. In the present study, we investigated the functional role of α1A ARs expressed by PDGFRα$^+$ cells in colonic motility. Several experimental approaches were used, including 1) morphological study of colonic musculatures, 2) gene expression study, 3) patch clamp technique to study isolated single PDGFRα$^+$ cell, 4) Ca^{2+} imaging of cells within intact muscle preparations, 5) measurements of the electrical and contractile behaviors of intact colonic muscles, and 6) studies of colonic motility using whole colon preparations with the lumber colonic nerve (LCN) and the inferior mesenteric ganglion (IMG) intact. We also studied colonic motor activities in *Adra1a*$^{-/-}$ mice to test our hypothesis. Our results indicate that PDGFRα$^+$ cells are direct effectors for the motor responses of colonic muscle to sympathetic neural inputs. Post-synaptic responses are mediated by α1A ARs expressed by PDGFRα$^+$ cells, and this pathway is a primary and potent mechanism of sympathetic neural regulation in the murine colon.

In morphological study, the muscle layers of the mouse distal colon displayed considerable innervation by sympathetic nerve fibers, as has also been reported in the rat small intestine (31). Tyrosine-hydroxylase (TH)$^+$ fibers consist of sympathetic nerve fibers and enteric dopaminergic nerve fibers, but most of TH$^+$ fibers represent sympathetic nerve fibers because dopaminergic neurons are very sparse (32). PDGFRα$^+$ cells and sympathetic nerve fibers were found to be in close proximity, suggesting that this class of interstitial cells could be targets for sympathetic neurotransmission. In the SIP syncytium α1 ARs are expressed exclusively in PDGFRα$^+$ cells according to cell-specific transcriptome data (10–12). However, the distribution of α1 ARs in mouse colon was not revealed morphologically, because of the lack of specific antibodies against α1 ARs (33). Indeed, we checked two anti-α1A AR antibodies (Santa Cruz Biotechnology; SC-1477 and Thermo Fisher SCIENTFIC; PA1–047) and observed no specific staining in the GI tract with either reagent, as compared to negative controls with primary antibodies omitted (data not shown). Therefore, by using other methods, we acquired evidence supporting the hypothesis that α1 ARs are enriched in PDGFRα$^+$ cells. Gene expression study using qPCR showed that the gene transcripts of α1 ARs (*Adra1a* and *Adra1b*) were greatly enriched in PDGFRα$^+$ cells (Fig. 1B). Enteric neurotransmitter antagonists did not affect the inhibitory responses to SNS mediated by α1 ARs in muscles of the distal colon. This suggests that functional expression of α1 ARs by enteric neurons is not responsible for the motor effects of SNS (Supplementary Fig. 2). Therefore, we concluded that α1 ARs expressed by PDGFRα$^+$ cells compose an important component of sympathetic response in mouse colon.

We previously reported techniques to isolate PDGFRα$^+$ cells and reported electrophysiological properties of these cells (14, 17). In the present study, we studied electrical responses of PDGFRα$^+$ cells to α1 AR agonists. NE activated K^+ conductance and hyperpolarized the membrane potential of PDGFRα$^+$ cells, and these effects were significantly inhibited by an α1A AR antagonist or an SK channel blocker, suggesting that the α1A AR-SK channel signal pathway operates in PDGFRα$^+$ cells (Fig. 1C–E). Activation of SK channels and hyperpolarization are linked to α1A ARs by generation of Ca^{2+} transients in PDGFRα$^+$ cells (Fig. 2). The hyperpolarization in PDGFRα$^+$ cells conducts to adjacent SMCs via gap junctions, resulting in hyperpolarization of SMCs (Fig. 3), leading to inhibition of spontaneous phasic contractions (Fig. 4 and summarized in Fig. 7).

In most previous reports of colonic contractile responses, muscle preparations detached from sympathetic ganglia were used. Sympathetic responses to electrical field stimulation (EFS) are hardly detectable in preparations of this type, and thus the role of sympathetic regulation of colonic motility was not understood from these experiments. Therefore, we established whole colon preparations with the lumber colonic nerve (LCN) and the inferior mesenteric ganglion (IMG) intact to study the effects of SNS on colonic motility uncontaminated by direct stimulation of enteric motor neurons that occurred with EFS. In these preparations, SNS inhibited contractions of distal colon and blocked CMMCs via theα1A AR-SK channels signal pathway expressed by PDGFRα$^+$ cells. The inhibitory effects of SNS (2 Hz) on CMMCs were completely abolished by an α1A AR antagonist and did not observed in *Adra1a*$^{-/-}$ mice in the mid and distal colon, even though α2 and β ARs remained intact and accessible to NE. Furthermore, blocking cholinergic neurotransmission with atropine was less potent in inhibiting CMMCs than SNS (2Hz). These data indicate that sympathetic neurotransmission via the α1A AR-SK channels signal pathway in PDGFRα$^+$ cells is a primary mechanism in sympathetic neural regulation of colonic motility, which is in contrast to the long-held dogma that inhibition of cholinergic enteric motor neurons via α2 ARs is the dominant mechanism of sympathetic neural regulation of colonic motility (1, 2, 34, 35). Additionally, these data imply that sympathetic activity may generates constant tonic inhibition of colonic propulsive contractions through this novel pathway, because it has been reported that sympathetic nerve fibers display tonic firing at more than 2Hz (36). This novel pathway might have an important role for colonic accommodation under stress.

The differences of the potency of inhibitory effects of SNS on CMMC in different regions of colon suggest that sympathetic innervation originating from IMG may be primarily in the mid and distal colon. Sympathetic innervation of the proximal colon may originate primarily from the superior mesenteric ganglion (SMG). However, because inhibition of CMMCs by stimulating IMG occurs to some extent in the proximal colon (Fig. 6E), some of the neurons from IMG may also innervate the proximal colon. In this study, we focused on the effects of neurons of IMG and did not study the effects of neurons of SMG. It is of course possible that neurons of SMG might have a different role in regulating the motility of the proximal colon compared to neurons of IMG. This possibility will require further experiments in the future.

In conclusion, this study revealed a novel population of cells that mediate an important component of sympathetic neural regulation of murine colonic motility. From our studies on mouse, the α1A AR-SK channel signal pathway in PDGFRα$^+$ cells appears to be the dominant means of conveying sympathetic neural regulation to the colonic musculature. We have found a similar population of PDGFRα$^+$ cells in human colonic muscles (37). Human colonic PDGFRα$^+$ cells also express SK3 channels, and muscles display inhibitory junction potentials activated by stimulation of intrinsic enteric inhibitory neurons and mediated by P2Y1 receptors and an apamin-sensitive SK conductance (37, 38). Therefore, it is possible that the α1A AR-SK channel signal pathway which we identified in murine PDGFRα$^+$ cells could also be present in the human colon. This novel regulatory pathway may contribute to stress responses experienced by human patients that exacerbate the symptoms of functional bowel disorders, such as IBS (39). Previous studies have shown that patients with IBS have higher concentrations of plasma NE than healthy controls (40, 41). Thus, α1A AR selective antagonists might prove to be tools to blunt the effects of stress on colonic motility.

Supplementary Material

Refer to Web version on PubMed Central for supplementary material.

Acknowledgements

We would like to thank Dr. Retsu Mitsui in Nagoya City University for helping the immunohistochemistry about α1A adrenoceptors.

This work was supported by National Institute of Diabetes and Digestive and Kidney Diseases (NIDDK) Grant R01-DK-091336.

Nonstandard Abbrebiations

ALMH	atropine (1 μM) + L-NNA (100 μM) + MRS2500 (1 μM) + Hexamethonium (100 μM)
ARs	adrenoceptors
AUC	area under the curve
CM	circular muscle
CMMCs	colonic migrating motor complexes
EFS	electrical field stimulation
Epi	epinephrine
ER	endoplasmic reticulum
FBD	functional bowel disorders
FACS	fluorescence activated cell sorting
GPCR	G-protein coupled receptors

IBS	irritable bowel syndrome
ICC	interstitial cells of Cajal
IMG	the inferior mesenteric ganglion
IP3	inositol triphosphate
LCN	the lumber colonic nerve
L-NNA	N-Nitro-L-arginine methyl ester hydrochloride
NE	norepinephrine
PDGFRα+ cells	platelet-derived growth factor receptor α^+ cells
PE	phenylephrine
PLC	phospholipase C
SIP syncytium	SMCs, ICC and PDGFRα^+ cells syncytium
SK channels	small conductance Ca^{2+}-activated K^+ channels
SMCs	smooth muscle cells
SNS	sympathetic nervous system
SPCs	spontaneous phasic contractions; TH: tyrosine hydroxylase
TTX	tetrodotoxin
WT	wild type

References

1. Norberg KA and Sjoqvist F (1966) New possibilities for adrenergic modulation of ganglionic transmission. Permacol. Rev 18, 743–751
2. Burnstock G and Costa M (1973) Inhibitory innervation of the gut. Gastroenterology 64, 141–144 [PubMed: 4683851]
3. De Ponti F, Giaroni C, Cosentino M, Lecchini S and Frigo G (1996) Adrenergic mechanisms in the control of gastrointestinal motility: from basic science to clinical applications. Pharmacol. Ther 69, 59–78 [PubMed: 8857303]
4. Lomax AE, Sharkey KA and Furness JB (2010) The participation of the sympathetic innervation of the gastrointestinal tract in disease states. Neurogastroenterol. Motil 22, 7–18 [PubMed: 19686308]
5. Gagnon DJ, Devroede G. and Belisle S. (1972) Excitatory effects of adrenaline upon isolated preparations of human colon. Gut 13, 654–657 [PubMed: 5077177]
6. Sanders KM, Koh SD, Ro S and Ward SM (2012) Regulation of gastrointestinal motility-insights from smooth muscle biology. Nat. Rev. Gastroenterol. Hepatol 9, 633–645 [PubMed: 22965426]
7. Sanders KM, Kito Y, Hwang SJ and Ward SM (2016) Regulation of gastrointestinal smooth muscle function by interstitial cells. Physiology 31, 316–326 [PubMed: 27488743]
8. Komuro T, Seki K and Horiguchi K (1999) Ultrastructural characterization of the interstitial cells of Cajal. Arch. Histol. Cytol 62, 295–316 [PubMed: 10596941]

9. Iino S, Horiguhci K, Horiguchi S and Nojyo Y (2009) c-Kit-negative fibroblast-like cells express platelet-derived growth factor receptor alpha in the murine gastrointestinal musculature. Histochem. Cell Biol 131, 691–702 [PubMed: 19280210]
10. Lee MY, Park C, Berent RM, Park PJ, Fuchs R, Syn H, Chin A, Townsend J, Benson CC, Redelman D, Shen TW, Park JK, Miano JM, Sanders KM and Ro S (2015) Smooth muscle cell genome browser: Enabling the identification of novel serum responce factor target genes. PLoS One 10, e0133751 [PubMed: 26241044]
11. Lee MY, Ha SE, Park C, Park PJ, Fuchs R, Wei L, Jorgensen BG, Redelman D, Ward SM, Sanders KM and Ro S (2017) Transcriptome of interstitial cells of Cajal reveals unique and selective gene signature. PLoS One 12, e0176031 [PubMed: 28426719]
12. Ha SE, Lee MY, Kurahashi M, Wei L, Jorgensen BG, Park C, Park PJ, Redelman D, Sasse KC, Becker LS, Sanders KM and Ro S (2017) Transcriptome analysis of PDGFRα+ cell hyperplasia. PLoS One 12, e0182265 [PubMed: 28806761]
13. Piascik MT and Perez DM (2001) Alpha1-adrenergic receptors: new insights and directions. J. Pharmacol. Exp. Ther 298, 403–410 [PubMed: 11454900]
14. Kurahashi M, Zheng H, Dwyer L, Ward SM, Koh SD and Sanders KM (2011) A functional role for the ‘fibroblast-like cells’ in gastrointestinal smooth muscles. J. Physiol 589, 697–710 [PubMed: 21173079]
15. Hwang SJ, Blair PJ, Durnin L, Mutafova-Yambolieva V, Sanders KM and Ward SM (2012) P2Y1 purinoreceptors are fundamental to inhibitory motor control of murine colonic excitability and transit. J. Physiol 590, 1957–1972 [PubMed: 22371476]
16. Peri LE, Sanders KM and Mutafova-Yambolieva VN (2013) Differential expression of genes related to purinergic signaling in smooth muscle cells, PDGFRα-positive cells, and interstitial cells of Cajal in the murine colon. Neurogastroenterol. Mtil 25, e609–620
17. Kurahashi M, Mutafova-Yambolieva V, Koh SD and Sanders KM (2014) Platelet-derived growth factor receptor-α-positive cells and not smooth muscle cells mediate purinergic hyperpolarization in murine colonic muscles. Am. J. Physiol. Cell Physiol 307, C561–C570 [PubMed: 25055825]
18. Baker SA, Henning GW, Salter AK, Kurahashi M, Ward SM and Sanders KM (2013) Distribution and Ca(2+) signaling of fibroblast-like (PDGFR(+)) cells in the murine gastric fundus. J. Physiol 591, 6193–6208 [PubMed: 24144881]
19. Hamilton TG, Klinghoffer RA, Corrin PD and Soriano P (2003) Evolutionary divergence of platelet-derived growth factor alpha receptor signaling mechanisms. Mol. Cell Biol 23, 4013–4025 [PubMed: 12748302]
20. Koh SD, Dick GM and Sanders KM (1997) Small-conductance Ca^{2+}-dependent K^{+} channels activated by ATP in murine colonic smooth muscle. Am. J. Physiol. Cell Physiol 273, C2010–C2021
21. Baker SA, Drumm BT, Skowronek KE, Rembetski BE, Peri LE, Hennig GW, Perrino BA and Sanders KM (2018) Excitatory neuronal responses of Ca2+ transients in interstitial cells of Cajal in the small intestine. eNeuro 5, ENEURO.0080–18
22. Baker SA, Drumm BT, Saur D, Hennig GW, Ward SM and Sanders KM (2016) Spontaneous Ca(2+) transients in interstitial cells of Cajal located within the deep muscular plexus of the murine small intestine. J. Physiol 594, 3317–3338 [PubMed: 26824875]
23. Spencer NJ, Bywater RA and Klemm MF (1998) Effects of sympathetic nerve stimulation on membrane potential in the circular muscle layer of mouse distal colon. Neurogastroenterol. Motil 10, 543–552 [PubMed: 10050260]
24. Williams TJ, Blue DR, Daniels DV, Davis B, Elworthy T, Gever JR, Kava MS, Morgans D, Padilla F, Tasse S, Vimont RL, Chapple CR, Chess-Williams R, Rglen RM, Charke DE and Ford AP (1999) In vitro alpha1-adrenoceptor pharmacology of Ro 70–0004 and RS-100329, novel alpha1A-adrenoceptor selective antagonists. Br. J. Pharmacol 127, 252–258 [PubMed: 10369480]
25. Baker SA, Hennig GW, Ward SM and Sanders KM (2015) Temporal sequence of activation of cells involved in purinergic neurotransmission in the colon. J Physiol 593, 1945–1963 [PubMed: 25627983]
26. Chhatriwala M, Ravi RG, Patel RI, Boyer JL, Jacobson KA and Haden TK (2004) Induction of novel agonist selectivity for the ADP-activated P2Y1 receptor versus the ADP-activated P2Y12

and P2Y13 receptors by conformational constraint of an ADP analog. J. Pharmacol. Exp. Ther 311, 1038–1043 [PubMed: 15345752]

27. Spencer NJ, Dinning PG, Brookes SJ and Costa M (2016) Insights into the mechanisms underlying colonic motor patterns. J. Physiol 594, 4099–4226 [PubMed: 26990133]
28. Smith TK and Koh SD (2017) A model of the enteric neural circuitry underlying the generation of rhythmic motor patterns in the colon: the role of serotonin. Am. J. Gastrointest. Liver Physiol 312, G1–G14
29. Gonella J, Bouvier M and Blanquet F (1987) Extrinsic nervous control of motility of small and large intestines and related sphincters. Physiol. Rev 67, 902–961 [PubMed: 3299412]
30. Aggarwal A, Cutts TF, Abell TL, Cardoso S, Familoni B, Bremer J and Karas J (1994) Predominant symptoms in irritable bowel syndrome correlate with specific autonomic nervous system abnormalities. Gastroenterology 106, 945–950 [PubMed: 8143999]
31. Walter GC, Phillips RJ, McAdams JL and Powley TL (2016) Individual sympathetic postganglionic neurons coinnervate myenteric ganglia and smooth muscle layers in the gastrointestinal tract of the rat. J. Comp. Neurol 524, 2577–2603 [PubMed: 26850701]
32. Anderson G, Noorian AR, Taylor G, Anitha M, Bernhard D, Srinivasan S and Greene JG (2007) Loss of enteric dopaminergic neurons and associated changes in colon motility in an MPTP mouse model of Parkinson's disease. Exp. Neurol 207, 4–12 [PubMed: 17586496]
33. Pradidarcheep W, Stallen J, Labruyere WT, Dabhoiwala NF, Michel MC and Lamers WH (2009) Lack of specificity of commercially available antisera against muscarinergic and adrenergic receptors. Naunyn. Schmiedebergs Arch. Pharmacol 379, 397–402 [PubMed: 19198807]
34. Manber L and Gershon MD (1979) A reciprocal adrenergic-cholinergic axoaxonic synapse in the mammalian gut. Am. J. Physiol 236, 738–745
35. Furness JB, Callaghan BP, Rivera LR and Cho HJ (2014) The enteric nervous system and gastrointestinal innervation: integrated local and central control. Adv. Exp. Med. Biol 817, 39–71 [PubMed: 24997029]
36. McAllen RM and Malpas SC (1997) Sympathetic burst activity: characteristics and significance. Clin. Exp. Pharmacol. Physiol 24,791–799 [PubMed: 9363359]
37. Kurahashi M, Nakano Y, Hennig GW, Ward SM. and Sanders KM. (2012) Platelet-derived growth factor receptor α-positive cells in the tunica muscularis of human colon. J. Cell. Mol. Med 16, 1397–1404 [PubMed: 22225616]
38. Gallego D, Hernandez P, Clave P. and Jimenez M. (2006) P2Y1 receptors mediate inhibitory purinergic neuromuscular transmission in the human colon. Am. J. Physiol. Gastrointest. Liver Physiol 291, G584–594 [PubMed: 16751171]
39. Ford AC, Lacy BE and Talley NJ (2017) Irritable Bowel Syndrome. N. Engl. J. Med 376, 2566–2578 [PubMed: 28657875]
40. Berman S, Suyenobu B, Naliboff BD, Bueller J, Stains J, Wong H, Mandelkern M, Fitsgerald L, Ohning G, Gupta A, Labus KS, Tillisch K and Mayer EA (2012) Evidence for alterations in central noradrenergic signaling in irritable bowel syndrome. Neuroimage 63, 1854–1863 [PubMed: 22917679]
41. Posserud I, Agerforz P, Ekman R, Bjornsson ES, Abrahamsson H and Simren M (2004) Altered visceral perceptual and neuroendocrine response in patients with irritable bowel syndrome during mental stress. Gut. 58, 1102–1108

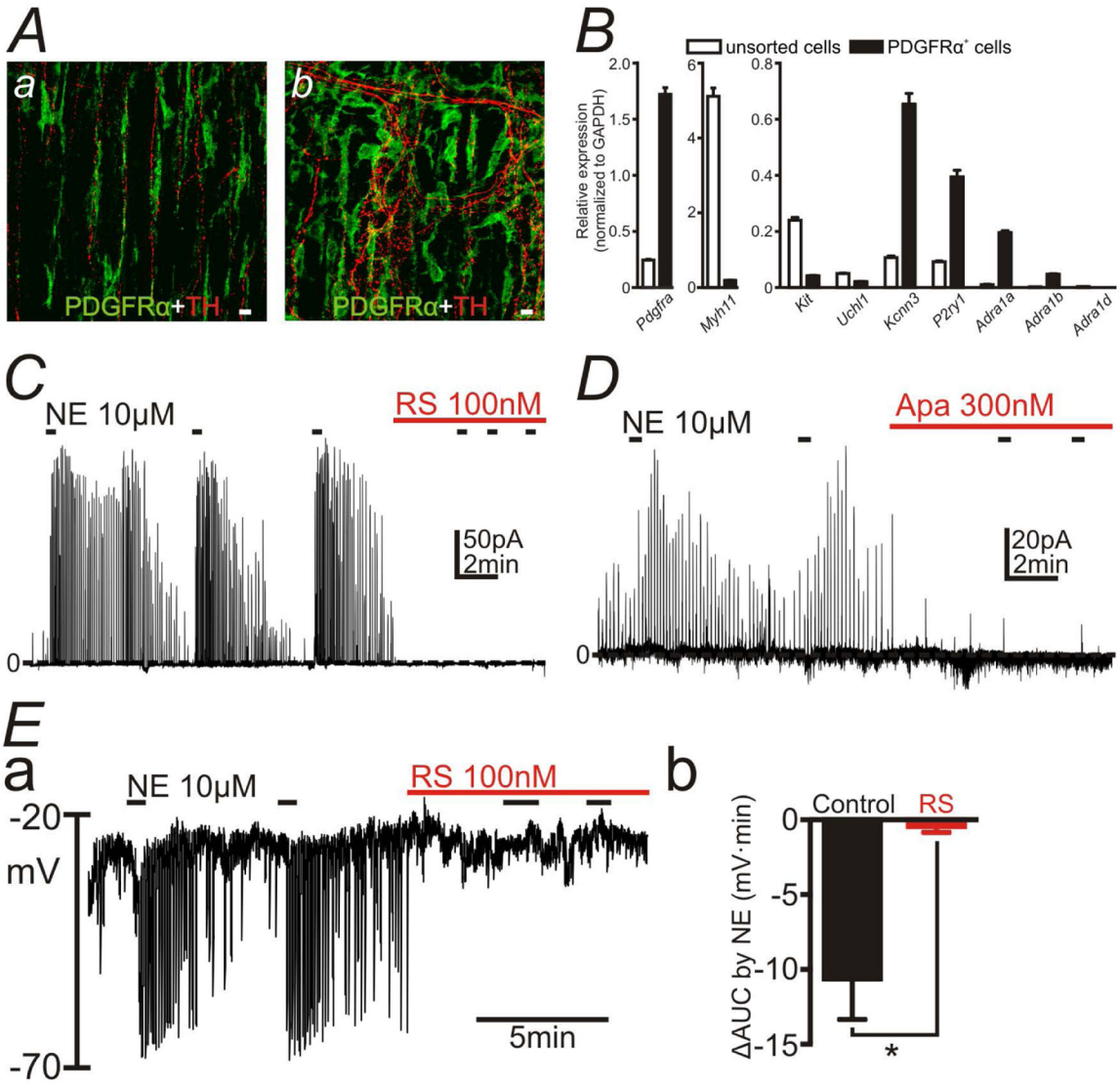

Figure 1:

Capability of PDGFRα$^+$ cells to responding to sympathetic neural signaling. **A:** Whole tissue immunohistochemical labeling of PDGFRα (green) and tyrosine hydroxylase (TH) (red) in circular muscle layer (a) and plane of the myenteric plexus (b) in the mouse distal colon. PDGFRα$^+$ cells were closely associated with TH$^+$ varicose nerve fibers. White scale bars represent 10 μm. **B:** Gene expression in PDGFRα$^+$ cells and unsorted cells, which were the dispersed cells of colon before FACS, analyzed by qPCR. α1 Adrenoceptors (ARs) (*Adra1a*, *Adra1b* and *Adra1d*), especially *Adra1a* were expressed in PDGFRα$^+$ cells. **C-E:** Patch clamp data to PDGFRα$^+$ cells. Norepinephrine (NE; 10 μM) was applied repetitively (black bars). NE evoked transient outward currents in voltage-clamp mode at the holding potential of −50 mV (C and D). NE caused transient hyperpolarization in current-clamp mode ($I = 0$) in PDGFRα$^+$ cells (Ea). Outward currents and hyperpolarization responses evoked by NE were blocked by RS100329 (RS; 100nM) (C and E) or apamin (Apa; 300nM) (D). Eb summarizes ΔAUC (mV·min) (AUC for 1 min after applying NE - AUC for 1min

before applying NE) in the absence or the presence of RS in the current-clamp mode. * $P = 0.0084$.

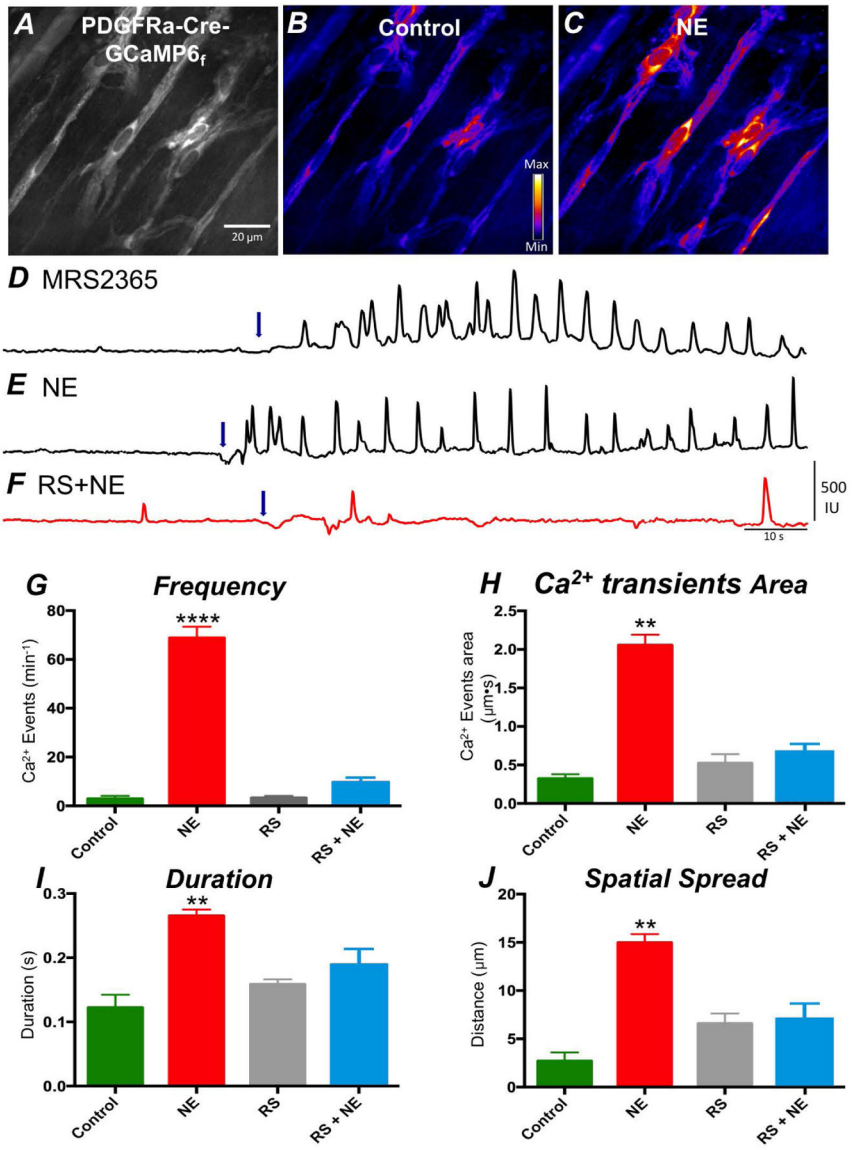

Figure 2:

Ca^{2+} transients in response to NE in PDGFRα^{+} cells. **A** Representative raw image showing PDGFRα cells in the intramuscular region of the colon expressing the Ca^{2+} sensor, $GCaMP6_f$. A purple hue was added as an overlay to enhance visualization in **B**; color scale indicates intensity of Ca^{2+} transients (i.e. dark blue is low florescence; light yellow to white indicate high florescence levels). **C** Image showing enhanced Ca^{2+} transients in PDGFRα^{+} cells in response to NE (10 μM). Scale bar in A is 20 μm and pertains to all images. **D** Representative traces showing Ca^{2+} transient activity in PDGFRα^{+} cells elicited by MRS2365 (P2Y1 receptor specific agonist; 1 μM). This is considered a signature response that identifies PDGFRα^{+} cells. **E** Representative Ca^{2+} transient activity in PDGFRα^{+} cells in response to NE (10 μM). **F** Ca^{2+} responses to NE were inhibited by RS100329 (100 nM, red trace). Arrows (blue) in D, E and F indicate points of NE application. **G** Frequency, **H** Ca^{2+} transient area, **I** duration and **J** spatial spread. * denotes significant difference between

control and after NE application. The numbers of asterisks mean: * 0.05 > $P \geq 0.01$; ** 0.01 > $P \geq 0.001$; *** 0.001 > $P \geq 0.0001$; **** 0.0001 > P.

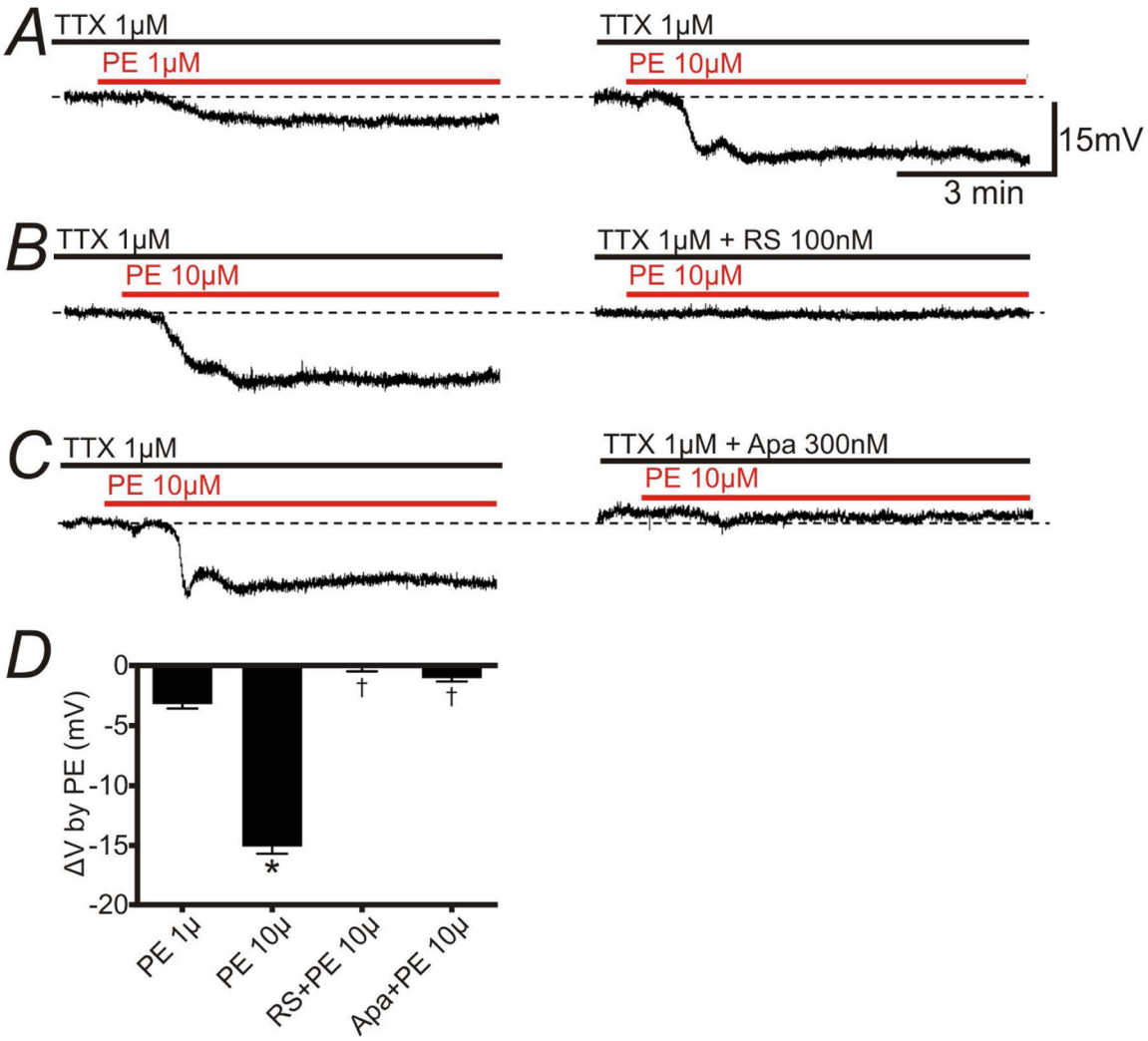

Figure 3:

Effects of Phenylephrine (PE) on membrane potentials recorded from circular SMCs of mouse distal colon. Intracellular recordings were performed in the presence of TTX (1 μM) to inhibit neural activity. **A:** PE (1 and 10 μM) induced a hyperpolarization. **B:** PE-induced hyperpolarization was abolished by pretreatment of RS100329 (100nM). C: Apamin (Apa) 300nM inhibited PE-induced hyperpolarization. The resting membrane potentials were: A: −47 mV; B: −42 mV; C: −46 mV. A-C were recorded from different tissues. Each record in a given set of two was obtained from the same impalement. D: Summary showing the effects of RS100329 and Apa on PE-induced hyperpolarization. * $P < 0.0001$, significant difference from ΔV of PE (1 μM).† $P < 0.0001$, significant difference from ΔV of PE (10 μM).

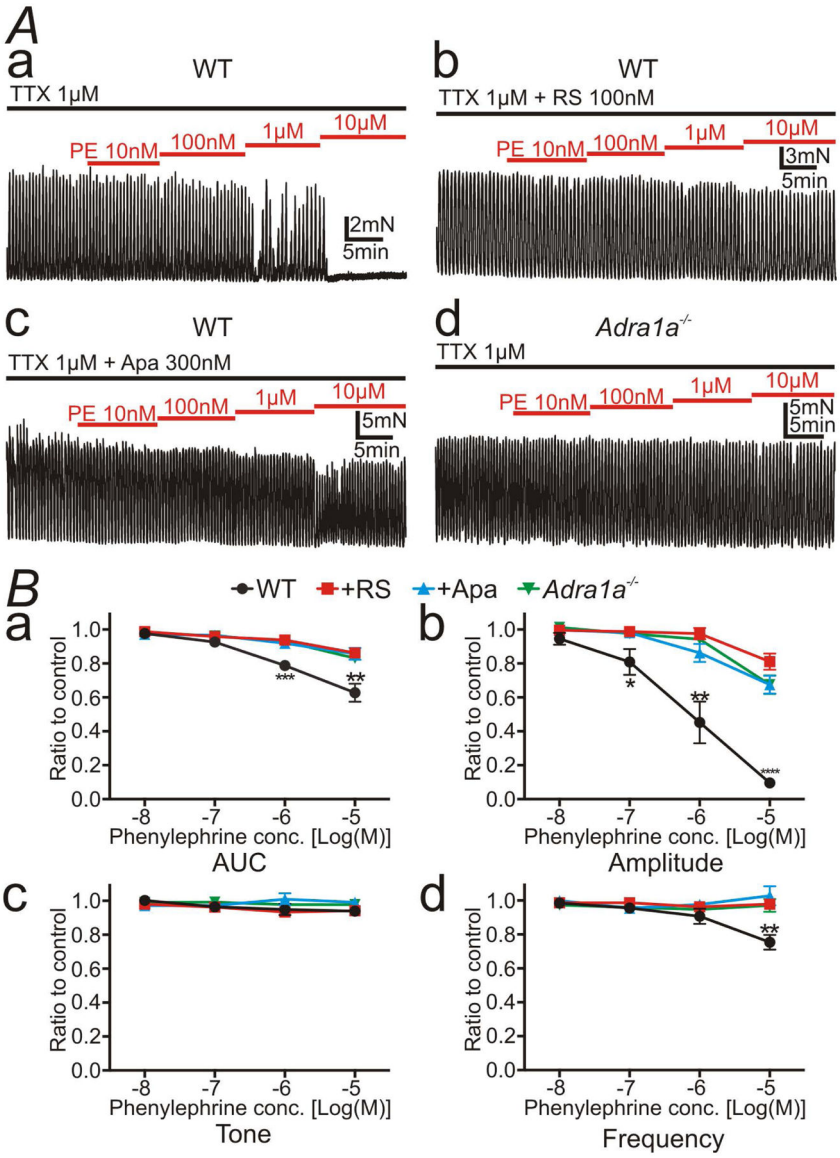

Figure 4:

Spontaneous phasic contractions (SPCs) of distal colonic circular muscle in the presence of tetrodotoxin (TTX; 1 μM). **A:** Phenylephrine (PE), a selective α1 AR ligand, inhibited SPCs in a concentration-dependent manner (Aa). RS100329 (RS; 100nM) (Ab), apamin (Apa; 300nM) (Ac), or the deletion of the gene encoding α1A ARs (Ad) inhibited the effects of PE. **B:** Summary of 4 contractile parameters, area under the curve (AUC) (Ba), amplitude (Bb), tone (Bc), and frequency (Bd) were tabulated as the ratio of SPCs before application of PE (control) to after application of PE. Amplitude of SPCs was most explicitly inhibited by PE alone compared to those in the presence of RS, apamin, or in the colonic muscles of *Adra1a*−/− mouse (Bb). * denote significant difference between PE alone and the other protocol. The numbers of asterisks mean the same as those in Fig. 2.

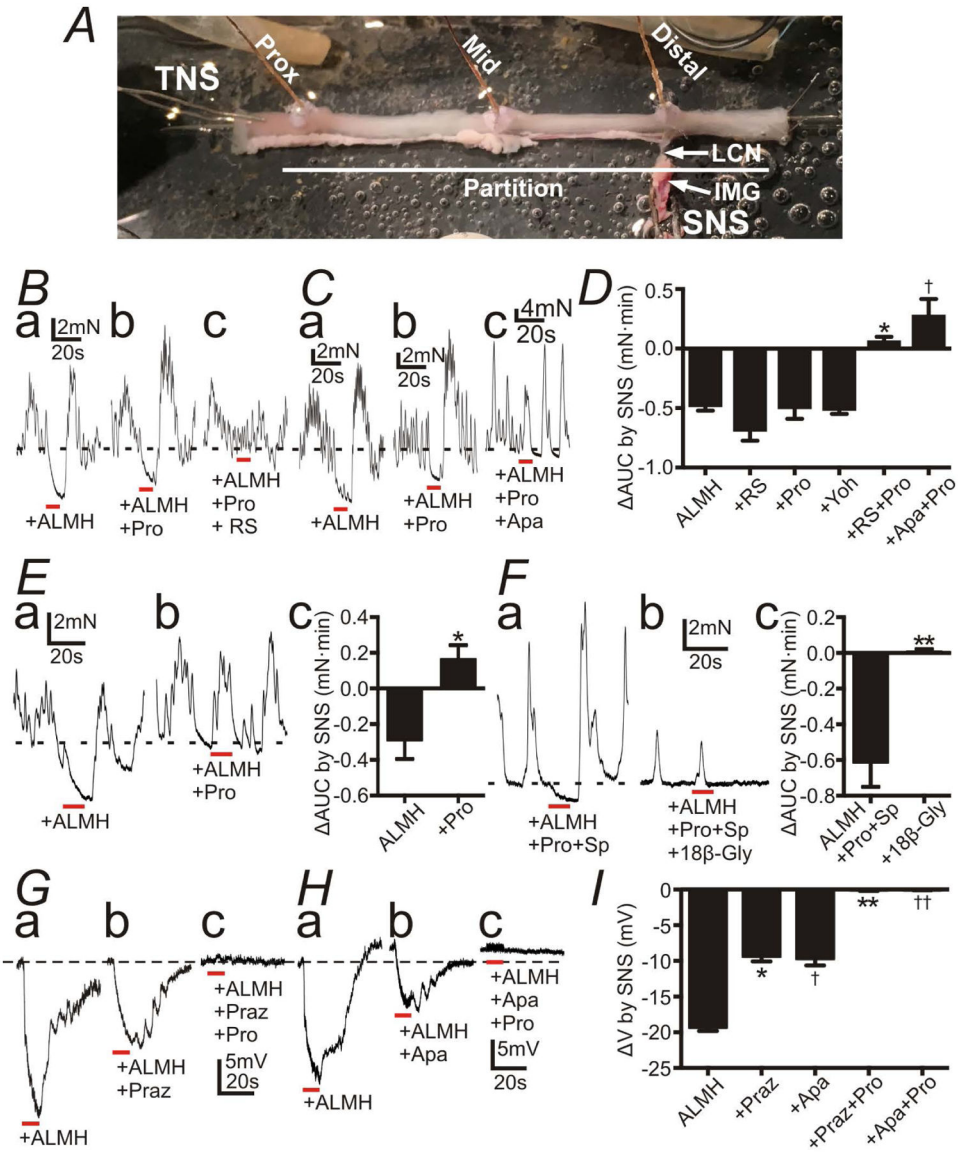

Figure 5:

Responses of the distal colon to sympathetic nerve stimulation (SNS) with atropine (1 μM) (A), L-NNA (100 μM) (L), MRS2500 (1 μM) (M), hexamethonium (100 μM) (H) (ALMH) in the bath solution. All red bars represent SNS at 20 Hz at 150 V for 10 s (pulse duration: 0.3 ms). All black dot-lines represent the control baseline of contractions or the resting membrane potentials. **A:** A preparation for the tension recordings with the lumber colonic nerve (LCN) and the inferior mesenteric ganglion (IMG) intact. **B and C:** Contractile experiments of WT mouse. SNS caused inhibition of contractions (Ba and Ca). Propranolol (Pro; 10 μM) didn't block inhibitions by SNS (Bb and Cb), but Pro+ RS100329 (RS; 100 nM) (Bc) or + apamin (Apa; 300nM) (Cb) blocked them (Bc and Cc). **D:** Summary of ΔAUC (mN•min) by SNS (AUC during SNS - the 10s average of AUC before SNS). * and† $P < 0.0005$, significant difference from ΔAUC with any single reagent. **E:** Contractile experiments of *Adra1a*$^{-/-}$ mouse. SNS relaxed distal colon (Ea) and Pro blocked inhibitions

by SNS (Eb). Ec shows summary of ΔAUC (mN•min) by SNS. * $P < 0.05$. **F:** Contractile experiments of WT mouse with Pro and substance P (Sp; 1 μM). SNS relaxed distal colon (Fa). 18β-Glycyrrhetinic acid (18β-Gly; 100 μM) blocked inhibitions by SNS (Fb). Fc showed summary of ΔAUC (mN•min) by SNS. ** $P < 0.005$. **G-H:** Intracellular electrical recordings of SMCs of WT mouse. SNS induced fast and slow phases of hyperpolarization (Ga and Ha). Prazosin (Praz; 1 μM) or Apa inhibited the fast hyperpolarization (Gb and Hb), and Pro inhibited the residual slow hyperpolarization (Gc and Hc). Resting membrane potential were: G, −48 mV; H, −51mV. G and H were recorded from different tissues. Each record in a given set of three was obtained from the same impalement. **I:** Summary of ΔV (mV) (induced hyperpolarization by SNS). * and† $P < 0.0001$, significant difference from ΔV of control. ** and†† $P < 0.0001$, significant difference from Praz and Apa respectively.

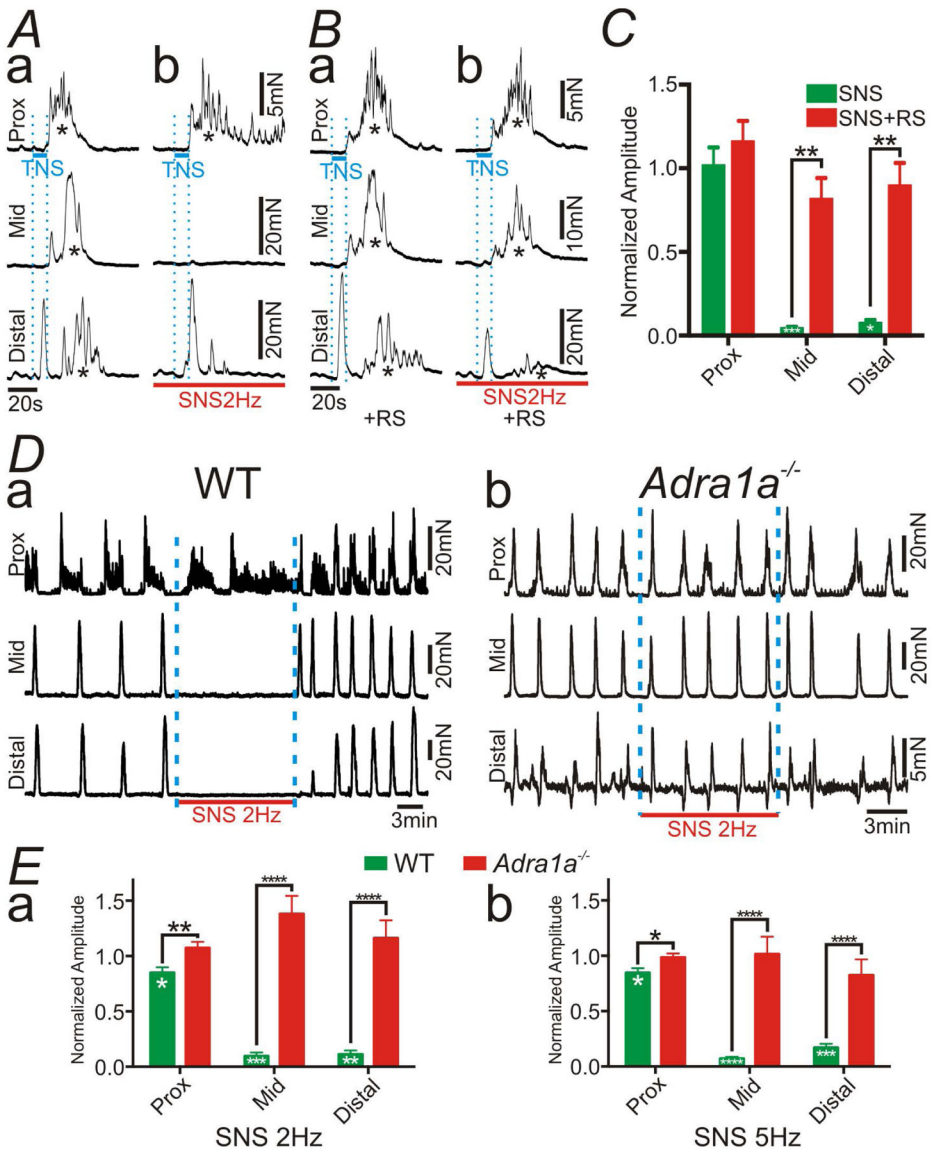

Figure 6:

Tension recordings at proximal (Prox), mid and distal colon in the preparation shown in Figure 5A. In this experiment, transmural nerve stimulation (TNS) across wall of proximal colon (blue bars in A and B) elicited the colonic migrating motor complex (CMMC; indicated by *). **A:** Sympathetic nerve stimulation (SNS; 2 Hz; red bars in A and B) inhibited CMMC at mid and distal colon (Ab). **B:** The inhibitory effects of SNS (2Hz) on CMMC were blocked by RS100329 (RS; 100nM) (Ba and c). **C:** Summary of normalized amplitude of CMMC with SNS. RS attenuated the inhibitory effects of SNS. **D:** Spontaneous CMMC were inhibited by SNS (2 Hz) in WT mouse (Da), however CMMC were not affected by SNS (2 Hz) in the colon of *Adra1a*$^{-/-}$ mouse (Db). **E:** Summary of normalized amplitude of CMMC with SNS at 2 Hz (Ea) and 5 Hz (Eb). Deletion of the gene encoding α1A ARs blocked the inhibitory effects of SNS. In panels of C and E, Black asterisks denote statistically significant differences between the values connected by black

lines and white asterisks mean statistically significant differences between the amplitude with SNS and the control. The numbers of asterisks mean the same as those in Fig. 2.

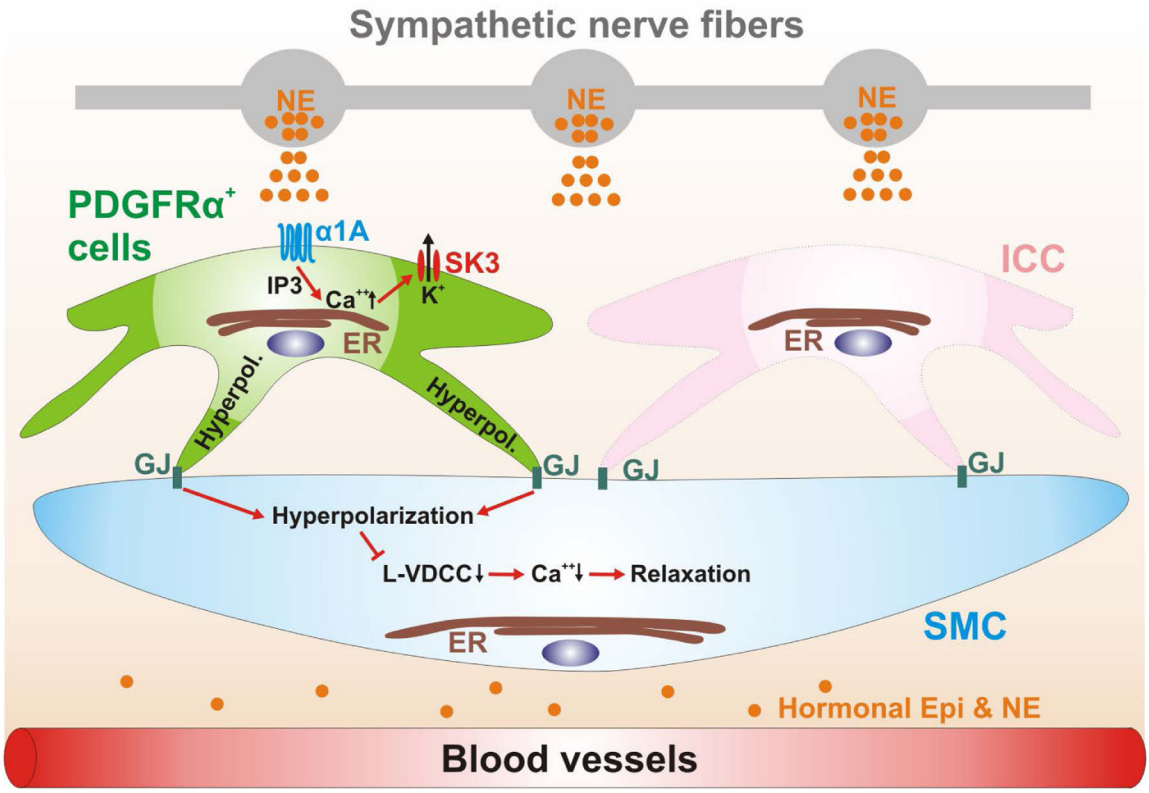

Figure 7:

Schematic diagram depicting a novel signal pathway of sympathetic neural regulation of murine colon. Sympathetic nerve fibers, a blood vessel and the cells of the SIP syncytium (SMCs, ICC and PDGFRα$^+$ cells) are displayed. Gap junctions (GJ) are shown between SMCs and ICC and PDGFRα$^+$ cells in dark green. PDGFRα$^+$ cells (pale green cell) express α1A ARs. Neuronal or hormonal norepinephrine (NE) (and possibly epinephrine; Epi) (orange circles) bind to α1A ARs, enhance Ca^{2+} release from endoplasmic reticulum (ER) via generation of inositol triphosphate (IP3) and activate small conductance Ca^{2+} -activated K^+ channels type 3 (SK3; expressed robustly in PDGFRα$^+$ cells; Fig. 1B). SK3 channels generate outward currents and induce hyperpolarization (Hyperpol.) in PDGFRα$^+$ cells, which conducts via GJ to SMCs (pale blue cell) and probably ICC (pink cell). Hyperpolarization of SMCs reduces the open probability of L-type Ca^{2+} channels (L-VDCC) and decreases intracellular [Ca^{2+}], leading to inhibition of contractions. ICC (pale pink cell) are not involved in this novel signal pathway.